ELSEVIER

www.elsevier.nl/locate/jorganchem

Journal of Organometallic Chemistry 620 (2001) 69–79

Journal of Organometallic Chemistry

Synthesis and structures of heterobimetallic Ir_2M (M=Pd, Pt) sulfido clusters and their catalytic activity for regioselective addition of alcohols to internal 1-aryl-1-alkynes

Dai Masui [a], Takuya Kochi [a], Zhen Tang [a], Youichi Ishii [a], Yasushi Mizobe [b], Masanobu Hidai [a,*,1]

[a] *Department of Chemistry and Biotechnology, Graduate School of Engineering, University of Tokyo, Hongo, Bunkyo-ku, Tokyo 113-8656, Japan*

[b] *Institute of Industrial Science, University of Tokyo, Roppongi, Minato-ku, Tokyo 106-8558, Japan*

Received 28 June 2000; received in revised form 30 August 2000; accepted 5 September 2000

Abstract

The heterobimetallic trinuclear sulfido clusters $[(Cp^*Ir)_2(\mu_3\text{-}S)_2MCl_2]$ (M = Pd (**3**), Pt (**4**); $Cp^* = \eta^5\text{-}C_5Me_5$) were synthesized from the dinuclear hydrogensulfido complex $[Cp^*IrCl(\mu\text{-}SH)_2IrCp^*Cl]$ (**2**) and $[MCl_2(COD)]$ (COD = cycloocta-1,5-diene), while the reaction of **2** with $[Pd(PPh_3)_4]$ afforded the cationic trinuclear cluster $[(Cp^*Ir)_2(\mu_3\text{-}S)_2PdCl(PPh_3)]Cl$ (**5**). Clusters **3** and **4** reacted with PPh_3 to give a series of mono and dicationic clusters including **5**, while the dicationic clusters $[(Cp^*Ir)_2(\mu_3\text{-}S)_2M(dppe)][BPh_4]_2$ (M = Pd (**9**), Pt (**10**); dppe = $Ph_2PCH_2CH_2PPh_2$) were obtained by the reaction with dppe followed by anion metathesis. The molecular structures of $\mathbf{5}\cdot CH_2Cl_2$, $\mathbf{9}\cdot CH_3COCH_3$, and $\mathbf{10}\cdot CH_3COCH_3$ were determined by X-ray crystallography. Clusters **3** and **4** were found to catalyze the addition of alcohols to alkynes to give the corresponding acetals. Internal 1-aryl-1-alkynes were transformed by cluster **3** into the corresponding 2,2-dialkoxy-1-arylalkanes with high regioselectivity up to 99:1, while cluster **4** was a much less regioselective catalyst.

Keywords: Palladium; Platinum; Iridium; Cluster; Catalytic addition; Crystal structure

1. Introduction

The chemistry of multinuclear transition metal complexes has recently been a subject of intensive research activity, because their multimetallic coordination sites are expected to facilitate unique chemical transformations through cooperative or successive interaction of the metal centers with substrate molecules [1]. In particular, multinuclear complexes with sulfur-based ligands are of special interest in connection with some biochemical reactions effected by metalloproteins and industrial processes by metal–sulfide catalysts [2], and a considerable number of metal–sulfur clusters containing first transition series metals and molybdenum have so far been synthesized and structurally characterized. In contrast, few studies on transition metal–sulfur multinuclear complexes toward organic synthesis have been performed [3], although they are anticipated to provide stable multimetallic reaction sites owing to the strong bridging ability of sulfur ligands to prevent fragmentation of the multimetallic cores. In this context, we have been engaged in developing multinuclear complexes of Groups 8–10 noble metals with bridging sulfur ligands and have uncovered, that such complexes in fact exhibit intriguing reactivities toward a wide variety of organic substrates [4–6]. One typical example is the cubane-type $PdMo_3S_4$ cluster $[PdMo_3(\mu_3\text{-}S)_4(tacn)_3Cl][PF_6]_3$ (**1**; tacn = 1,4,7-triazacyclononane), which behaves as an excellent catalyst for the stereoselective addition reactions of alcohols or carboxylic acids to electron defi-

* Corresponding author. Fax: +81-471-239362.

E-mail address: hidai@mail.rs.noda.sut.ac.jp (M. Hidai).

[1] Present address: Department of Materials Science and Technology, Faculty of Industrial Science and Technology, Science University of Tokyo, 2641 Yamazaki, Noda, Chiba 278-8510, Japan.

0022-328X/01/$ - see front matter
PII: S0022-328X(00)00619-7

cient alkynes and the lactonization of alkynoic acids [6]. The catalytic activities as well as the selectivities of cluster **1** in such reactions are far superior to those of conventional mononuclear palladium complexes. However, cluster **1** was not effective for the intermolecular addition of alcohols to nonactivated alkynes.

Recently, we have synthesized a series of dinuclear hydrogensulfido complexes such as [Cp*MCl(μ-SH)$_2$MCp*Cl] (M = Ru, Rh, Ir (**2**); Cp* = η^5-C_5Me_5) [7] and [Cp$_2$Ti(μ-SH)$_2$RuCp*Cl] (Cp = η^5-C_5H_5) [8] and demonstrated that they are used as versatile starting materials for the construction of homo and heterometallic, tri, tetra, and pentanuclear sulfido clusters containing the Cp*M(μ_3-S)$_2$MCp* unit(s) [7b,8,9]. In a previous communication, we have reported that the mixed-metal trinuclear clusters [(Cp*Ir)$_2$(μ_3-S)$_2$MCl$_2$] (M = Pd (**3**), Pt (**4**)) readily derived from complex **2** exhibit good catalytic activity for the addition of alcohols to nonactivated alkynes to give the corresponding acetals, and further, high regioselectivity is observed in the reactions of internal 1-aryl-1-alkynes by **3** [10]. Although a few transition metal compounds have been known to effect this type of addition of alcohols to alkynes [11], no regioselective catalyst has been developed for the reactions of internal alkynes. In this paper, we describe the synthesis and full characterization of the Ir$_2$M sulfido clusters (M = Pd, Pt) including **3** and **4** as well as the catalytic addition of alcohols to nonactivated alkynes by **3** and **4**.

2. Results and discussion

2.1. Synthesis and characterization of Ir_2M sulfido clusters (M = Pd, Pt)

When complex **2** was allowed to react with a small excess of [PdCl$_2$(COD)] (COD = cycloocta-1,5-diene) at 50°C in THF, the Ir$_2$Pd trinuclear cluster **3** was obtained in good yield as dark green crystals (Eq. (1)). A similar reaction of **2** with [PtCl$_2$(COD)] gave the analogous Ir$_2$Pt cluster **4**. Although single crystals of **3** and **4** suitable for crystallographic analysis could not be obtained, these clusters were characterized by spectroscopic and analytical data as well as X-ray diffraction studies of their phosphine derivatives (vide infra). In the ^{1}H-NMR spectrum of cluster **3**, only one singlet was observed at δ 2.15 attributable to the Cp* protons. A very similar ^{1}H-NMR spectrum with a singlet at δ 2.14 was obtained for cluster **4**. These data imply that in each case the COD ligand is replaced by the metalloligand Cp*Ir(μ_3-S)$_2$IrCp* derived from complex **2** to form the trinuclear cluster.

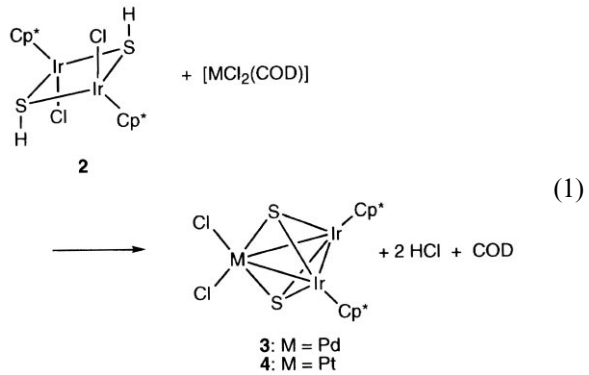

(1)

On the other hand, reaction of **2** with [Pd(PPh$_3$)$_4$] at room temperature (r.t.) afforded the cationic trinuclear cluster [(Cp*Ir)$_2$(μ_3-S)$_2$PdCl(PPh$_3$)]Cl (**5**) in 68% yield. In this case, the Pd(0) atom in [Pd(PPh$_3$)$_4$] is considered to be oxidized to the formal Pd(II) center of **5**. The GLC analysis of the gaseous phase indicated that H$_2$ was evolved during the reaction in 47% yield based on the complex **2** employed, which suggests the stoichiometry shown in Eq. (2). In the ^{1}H-NMR spectrum, cluster **5** exhibited one Cp* signal at δ 2.09 and Ph signals at δ 7.46–7.61 with the relative intensity ratio of 2:1. The ^{31}P{^{1}H}-NMR spectrum showing a singlet at δ 28.2 is also consistent with the formulation. In contrast, treatment of complex **2** with [Pt(PPh$_3$)$_4$] did not lead to the formation of the corresponding mixed-metal trinuclear cluster. The only cluster species identified by the ^{1}H-NMR analysis of the crude reaction mixture was the cubane-type tetrairidium cluster [(Cp*Ir)$_4$(μ_3-S)$_4$], which we previously described to be formed by treatment of **2** with a base [7c]. We have also observed that the hydrogensulfido-bridged diruthenium complex [Cp*RuCl(μ-SH)$_2$RuCp*Cl] reacts with [Pd(PPh$_3$)$_4$] to produce the tetranuclear cluster [(Cp*Ru)$_2${Pd(PPh$_3$)}$_2$-(μ_3-S)$_2$(μ-Cl)]Cl [12]. The structures of the cluster cores constructed from the dinuclear hydrogensulfido complexes are greatly affected by the combination of the metal elements involved.

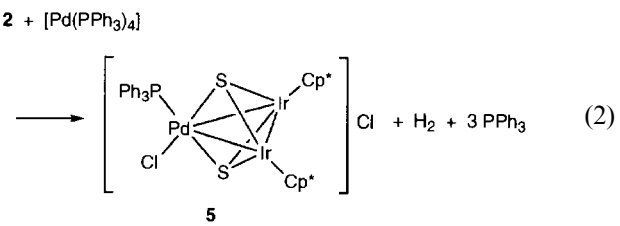

(2)

The molecular structure of **5**·CH$_2$Cl$_2$ was confirmed by X-ray diffraction study. An ORTEP drawing for the cationic part in **5**·CH$_2$Cl$_2$ is depicted in Fig. 1, and selected bond distances and angles are listed in Table 1. The cluster is composed of a 48 e$^-$ triangular core, which is capped by two μ_3-S ligands from both sides, and possesses a crystallographically imposed mirror plane containing the Pd(1), Cl(1), S(1), S(2), and P(1)

atoms. The palladium atom adopts a square planar geometry typical of a Pd(II) center. The Ir(1)–Ir(1*) and Ir(1)–Pd(1) distances are 2.9002(9) and 3.001(1) Å, respectively. Although the latter is longer than the reported Ir–Pd single bond distances including the distance (2.694(2) Å) in $[PdIr(CO)Cl(\mu\text{-dpmp})_2][PF_6]_2$ (dpmp = $PPh(CH_2PPh_2)_2$) [13], both Ir–Ir and Ir–Pd bonds are considered to have metal–metal bonding interactions in terms of the effective atomic number (EAN) rule. It is known that the divalent Group 10 metal atoms with the square planar geometry have a high-lying atomic p_z orbital perpendicular to the coordination plane, and its contribution to the metal–metal bonding is often small [14]. This may be the reason why the Ir–Pd bonds in **5** are elongated. The two μ_3-S ligands are unsymmetrically bound to the core with the different Pd–S bond distances (Pd(1)–S(1), 2.362(4); Pd(1)–S(2), 2.293(4) Å) because of the stronger *trans* influence of the phosphine ligand than that of the chloro ligand.

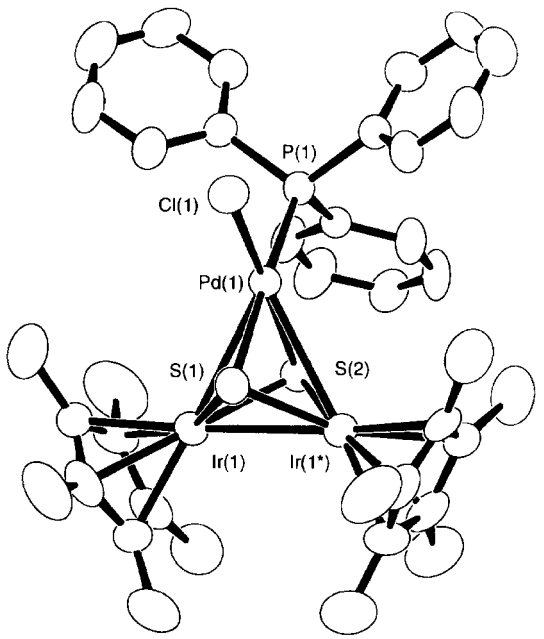

Fig. 1. Structure of the cationic part in **5**·CH_2Cl_2. Hydrogen atoms are omitted for clarity. Thermal ellipsoids are shown at the 50% probability level.

Table 1
Selected bond distances (Å) and angles (°) for **5**·CH_2Cl_2

Bond distances			
Ir(1)–Ir(1*)	2.9002(9)	Pd(1)–Cl(1)	2.346(4)
Ir(1)–Pd(1)	3.001(1)	Pd(1)–S(1)	2.362(4)
Ir(1)–S(1)	2.295(3)	Pd(1)–S(2)	2.293(4)
Ir(1)–S(2)	2.279(3)	Pd(1)–P(1)	2.281(4)
Bond angles			
Ir(1*)–Ir(1)–Pd(1)	61.11(1)	S(1)–Pd(1)–P(1)	175.9(1)
Ir(1)–Pd(1)–Ir(1*)	57.79(3)	S(2)–Pd(1)–P(1)	93.4(1)
S(1)–Ir(1)–S(2)	84.3(1)	Ir(1)–S(1)–Ir(1*)	78.4(1)
Cl(1)–Pd(1)–S(1)	93.3(1)	Ir(1)–S(1)–Pd(1)	80.2(1)
Cl(1)–Pd(1)–S(2)	175.8(1)	Ir(1)–S(2)–Ir(1*)	79.1(1)
Cl(1)–Pd(1)–P(1)	90.9(1)	Ir(1)–S(2)–Pd(1)	82.1(1)
S(1)–Pd(1)–S(2)	82.5(1)		

To gain additional information about the electronic state of the palladium center in cluster **3** and **5**, an XPS analysis was performed. The Pd-$3d_{5/2}$ binding energy for **3** was found to be 336.8 eV, which is considerably lower than those of the Pd(II) complexes including $[PdCl_2(PhCN)_2]$ (338.1 eV), $[PdCl_2(PPh_3)_2]$ (338.0 eV), and $[PdCl_2(PhSCH_2CH_2CH_2SPh)]$ (338.3 eV) but is somewhat higher than that of the Pd(0) complex $[Pd(PPh_3)_4]$ (335.9 eV), while the value for the cationic cluster **5** (337.8 eV) was not unusual as a Pd(II) species. The result of the XPS analysis suggests that the palladium center in **3** is substantially electron rich compared with those in common mononuclear Pd(II) complexes. The electron rich nature of the palladium center in **3** is reflected in the facile dissociation of the chloro ligand(s) to form cationic clusters by reaction with phosphines (vide infra). It should also be noted that the Pd-$3d_{5/2}$ binding energies for the cubane-type tetranuclear sulfido clusters **1** (336.0 eV) and $[\{Pd(PPh_3)\}_2\{Mo(S_2CNEt_2)\}_2(\mu_3\text{-}S)_4]$ (336.5 eV) [15] and the trinuclear cluster $[Pd(PPh_3)(\mu\text{-}S)_2\{Mo(S_2CNEt_2)\}_2(\mu\text{-}S)_2]$ (336.4 eV) [15] are close to that of **3**, although the oxidation states of the palladium atoms in these clusters still remain ambiguous. Thus, the palladium atom in **1** is regarded as Pd(0) rather than Pd(II) on the basis of the molecular orbital calculations [16], whereas the catalytic activities observed with **1** are diagnostic of a Pd(II) species [6b–d].

2.2. Reactions of clusters *3* and *4* with phosphine ligands

As described above, the Ir_2Pd cluster with a PPh_3 ligand **5** was prepared directly from complex **2**, whereas the analogous Ir_2Pt cluster could not be obtained by a similar synthetic method. We therefore investigated ligand substitution reactions of clusters **3** and **4** with phosphines. When nearly equimolecular amounts of cluster **3** and PPh_3 were dissolved in $CDCl_3$, the exclusive formation of cluster **5** was confirmed by ^1H- and $^{31}P\{^1H\}$-NMR. However, substitution of the second chloro ligand by excess PPh_3 occurred only to a minor extent. Thus, on treatment of **3** with 3.5 equivalents of PPh_3, a new species **6** showing a $^{31}P\{^1H\}$-NMR signal at δ 20.5 (s) emerged as the minor product (**5**:**6** = 73:27). This minor species **6** is tentatively formulated as the dicationic cluster $[(Cp^*Ir)_2(\mu_3\text{-}S)_2Pd(PPh_3)_2]Cl_2$, but attempts to isolate **6** in a pure form failed.

In contrast, the stepwise and complete conversion to the monosubstituted and disubstituted clusters was observed in the reaction of cluster **4** with PPh_3. Thus, on dissolving cluster **4** and one equivalent of PPh_3 in

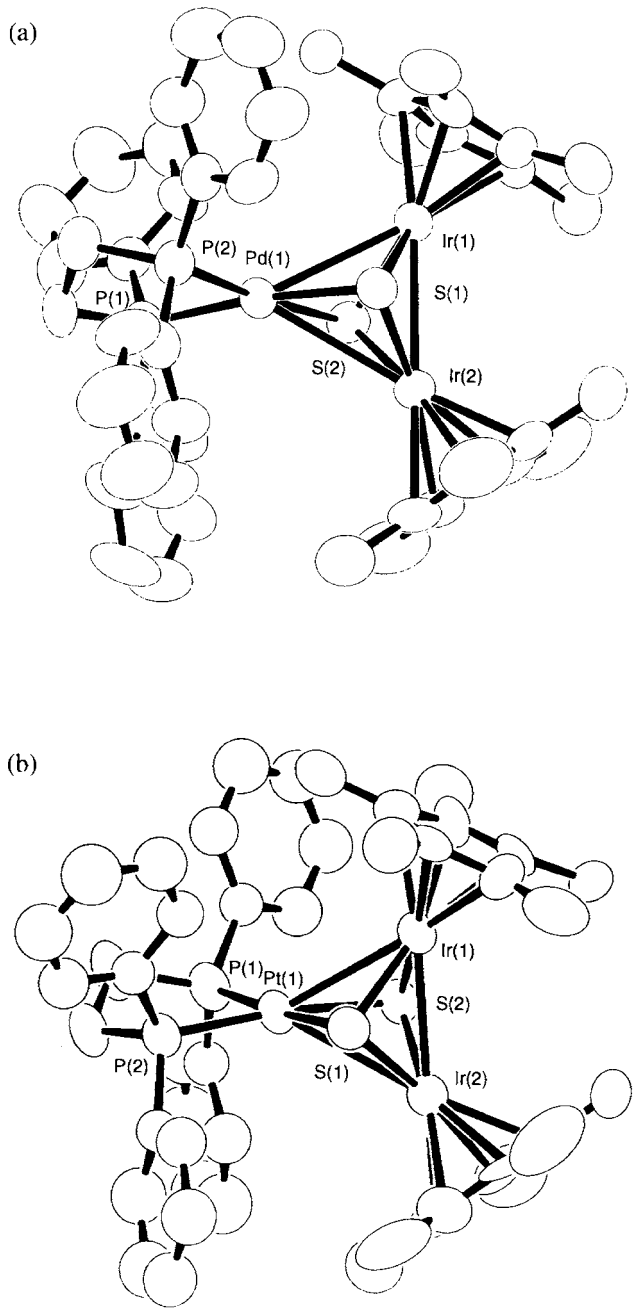

Fig. 2. Structures of the cationic parts in $9{\cdot}CH_3COCH_3$ (a) and $10{\cdot}CH_3COCH_3$ (b). Hydrogen atoms are omitted for clarity. Thermal ellipsoids are shown at the 50% probability level.

$CDCl_3$, a new complex showing singlets at δ 2.06 (Cp*) in the ^{1}H-NMR spectrum and at δ 12.7 ($J_{Pt-P} = 3945$ Hz) in the $^{31}P\{^1H\}$-NMR spectrum was formed as the major product. This species is characterized as the monocationic cluster $[(Cp^*Ir)_2(\mu_3\text{-}S)_2PtCl(PPh_3)]Cl$ (**7**) by analogy to the reaction of **3**. Further addition of one equivalent of PPh_3 to the above solution led to disappearance of cluster **7**, and the cluster $[(Cp^*Ir)_2(\mu_3\text{-}S)_2Pt(PPh_3)_2]Cl_2$ (**8**) was formed as the only detectable product, which exhibited singlets at δ 2.08 (Cp*) in the ^{1}H-NMR spectrum and at δ 2.9 ($J_{Pt-P} = 3685$ Hz) in the $^{31}P\{^1H\}$-NMR spectrum. Cluster **8** could be isolated as the $[BPh_4]^-$ salt $[(Cp^*Ir)_2(\mu_3\text{-}S)_2Pt(PPh_3)_2][BPh_4]_2$ (**8′**).

Treatment of **3** and **4** with 1.2 equivalents of dppe (dppe = $Ph_2PCH_2CH_2PPh_2$) caused spontaneous color change from green to purple, and further anion metathesis with $NaBPh_4$ afforded the dicationic clusters $[(Cp^*Ir)_2(\mu_3\text{-}S)_2M(dppe)][BPh_4]_2$ (M = Pd (**9**), Pt (**10**)) (Eq. (3)). The molecular structures of these clusters were unambiguously established by X-ray crystallography. ORTEP drawings for $\mathbf{9}{\cdot}CH_3COCH_3$ and $\mathbf{10}{\cdot}CH_3COCH_3$ are given in Fig. 2, and selected bond distances and angles are summarized in Table 2. Both clusters have a triangular core with two μ_3-S caps, which is closely related to that of cluster **5**. In each crystal, the two Ir–Pd (2.9532(9), 3.032(1) Å) or Ir–Pt (2.957(1), 3.038(1) Å) distances are not equivalent, but no special nonbonding interaction is observed within these cations. We consider that the inequality of the Ir–M distances is most probably due to crystal packing. These results provide additional support to the molecular structures of the Ir_2Pd and Ir_2Pt clusters **3** and **4**.

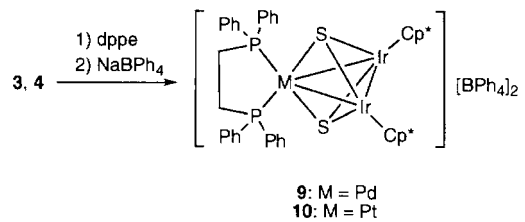

(3)

Table 2
Selected bond distances (Å) and angles (°) for $\mathbf{9}{\cdot}CH_3COCH_3$ and $10{\cdot}CH_3COCH_3$

	$\mathbf{9}{\cdot}CH_3COCH_3$ (M = Pd)	$10{\cdot}CH_3COCH_3$ (M = Pt)
Bond distances		
Ir(1)–Ir(2)	2.8758(9)	2.888(1)
Ir(1)–M(1)	2.9532(9)	2.957(1)
Ir(2)–M(1)	3.032(1)	3.038(1)
Ir(1)–S(1)	2.299(3)	2.298(4)
Ir(1)–S(2)	2.289(3)	2.309(5)
Ir(2)–S(1)	2.286(3)	2.301(5)
Ir(2)–S(2)	2.278(3)	2.303(5)
M(1)–S(1)	2.347(3)	2.362(5)
M(1)–S(2)	2.355(3)	2.347(4)
M(1)–P(1)	2.260(3)	2.256(5)
M(1)–P(2)	2.266(3)	2.252(4)
Bond angles		
Ir(2)–Ir(1)–M(1)	62.67(2)	62.61(3)
Ir(1)–Ir(2)–M(1)	59.91(2)	59.80(3)
Ir(1)–M(1)–Ir(2)	57.42(2)	57.58(3)
S(1)–Ir(1)–S(2)	85.42(9)	85.8(2)
S(1)–Ir(2)–S(2)	86.00(9)	85.9(2)
S(1)–M(1)–S(2)	82.89(9)	83.5(2)
S(1)–M(1)–P(1)	173.1(1)	175.6(2)
S(1)–M(1)–P(2)	95.9(1)	95.8(2)
S(2)–M(1)–P(1)	96.3(1)	95.6(2)
S(2)–M(1)–P(2)	175.1(1)	173.9(2)
P(1)–M(1)–P(2)	85.4(1)	85.5(2)

Table 3
Catalytic addition of MeOH to 1-phenyl-1-propyne [a]

Catalyst	Conversion (% [b])	Yield (% [c])	**12a**:**13a** [d]
$[(Cp^*Ir)_2(\mu_3\text{-}S)_2PdCl_2]$ (**3**)	>99	(88)	98:2
$[PdCl_2(PhSCH_2CH_2CH_2SPh)]$	28	0	
$[(Ph_3P)(PhS)Pd(\mu\text{-}SPh)]_2$	2.5	0	
$[Cp^*IrCl(\mu\text{-}SH)_2IrCp^*Cl]$ (**2**)	3	0	
$[IrCl(COD)]_2$	30	6	(35:65)
$[Cp^*IrCl(\mu\text{-}Cl)_2IrCp^*Cl]+[PdCl_2(COD)]$ [e]	33	0	
$[Pd(PPh_3)(\mu\text{-}S)_2\{W(S_2CNEt_2)\}_2(\mu\text{-}S)_2]$	2	0	
$[(Cp^*Ru)_2Pd_2(\mu_3\text{-}S)_2(SPr^i)(\mu\text{-}SPr^i)(PPh_3)]$	23	0	
$[(Cp^*Ir)_2(\mu_3\text{-}S)_2PtCl_2]$ (**4**)	>99	(96)	74:26
$[Pt(PPh_3)(\mu\text{-}S)_2\{W(S_2CNEt_2)\}_2(\mu\text{-}S)_2]$	1.5	0	

[a] For reaction conditions, see Section 3.
[b] Determined by GLC.
[c] GLC (isolated) yield.
[d] Determined by ^{1}H-NMR (GLC).
[e] 56 μmol each.

Reactions of **3** and **4** with other ligands such as CO and isocyanides were also investigated, but in most cases isolable products were not obtained. However, treatment of cluster **4** with an equimolecular amount of ^{t}BuNC followed by anion metathesis with KPF_6 yielded $[(Cp^*Ir)_2(\mu_3\text{-}S)_2PtCl(CN^tBu)][PF_6]$ (**11**). The IR spectrum of **11** exhibited a characteristic ν(CN) band at 2203 cm^{-1}, which is comparable to the values reported-for Pt(II) isocyanide complexes such as *trans*-$[Pt(C_3H_5)(C_5H_5)(CN^tBu)_2]$ (2188 cm^{-1}) [17]. Other spectral features of **11** as well as analytical data are in agreement with the formulation.

2.3. Catalytic addition of alcohols to alkynes

Having new Ir_2Pd and Ir_2Pt clusters **3** and **4** in hand, we turned our attention to their catalytic activity for the addition of alcohols to nonactivated alkynes. When phenylacetylene was allowed to react in MeOH at 50°C in the presence of a catalytic amount of **3**, two isomeric acetals, 1,1-dimethoxy-2-phenylethane and 1,1-dimethoxy-1-phenylethane, were formed in the ratio of 13:87 in 50% isolated total yield. A similar reaction of 1-octyne gave 2,2-dimethoxyoctane in 55% isolated yield as the sole product. In these reactions, the Markovnikov type products were obtained predominantly.

In contrast, the reaction of 1-phenyl-1-propyne with MeOH in the presence of cluster **3** gave rise to formation of 2,2-dimethoxy-1-phenylpropane (**12a**, $R^1 = R =$ Me, $R^2 = H$) and 1,1-dimethoxy-1-phenylpropane (**13a**, $R^1 = R = Me$, $R^2 = H$) in the ratio of 98:2 (Eq. (4)). No other products such as enol ethers and ketones were detected by GLC. Further purification of the products by column chromatography and bulb-to-bulb distillation afforded **12a** and **13a** in 88% combined yield. The highly selective formation of **12a** is of special interest. Several transition metal catalysts including $Na[AuCl_4]$ [11a], $[AuMe(PPh_3)]$–HOTf (OTf = OSO_2CF_3) [11b], $[PtCl_2(phosphine)_2]$–AgOTf [11c], and $[RuCl\{HB(pz)_3\}(COD)]$ (pz = pyrazol-1-yl) [11d] have been reported to effect the intermolecular addition of alcohols to nonactivated alkynes, but no regioselective reaction of internal alkynes has been observed. More recently, a ruthenium-catalyzed hydration of 1-alkynes to give the corresponding aldehydes has been reported [18]. However, this reaction is considered to proceed via a vinylidene complex and has not been applied to internal alkynes.

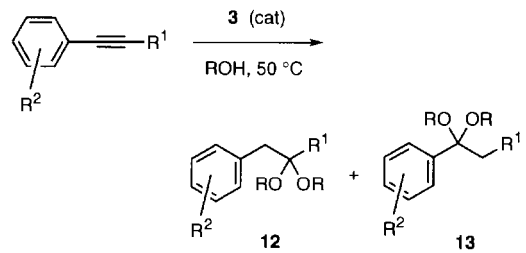

(4)

12a, **13a**: R = Me, R^1 = Me, R^2 = H
12b, **13b**: R = Et, R^1 = Me, R^2 = H
12c, **13c**: R = Me, R^1 = Et, R^2 = H
12d, **13d**: R = Me, R^1 = Bu^n, R^2 = H
12e, **13e**: R = Me, R^1 = Me, R^2 = *p*-Cl
12f, **13f**: R = Me, R^1 = Me, R^2 = *m*-Cl
12g, **13g**: R = Me, R^1 = Me, R^2 = *p*-Me
12h, **13h**: R = Me, R^1 = Me, R^2 = *p*-OMe

Various complexes related to **3** have been employed as the catalyst for the addition reaction of MeOH to 1,1-phenyl-1-propyne (Table 3). Neither monometallic palladium complexes with sulfur donor ligands nor iridium complexes including **2** were effective. The combined use of $[Cp^*IrCl(\mu\text{-}Cl)_2IrCp^*Cl]$ and $[PdCl_2(COD)]$ failed to show catalytic activity. In addition, it was confirmed that cluster **3** can be recovered in 85% yield after the catalytic reaction. On the basis of these results, we are inclined to believe that the catalysis is

performed not by the monometallic palladium or iridium species formed by fragmentation of cluster **3** but by the Ir_2Pd cluster whose core structure is retained during the reaction. On the other hand, the Ir_2Pt cluster **4** displayed good catalytic activity for the addition reaction, but the regioselectivity was much lower than that of **3**. Efforts to improve the catalytic activity of **3** by using an additive were not successful. Addition of PPh_3 or NEt_3 to the reaction mixture inhibited the catalytic activity of **3**. Several other heterobimetallic sulfido clusters containing palladium or platinum were also examined as the catalyst, but none of them showed good catalytic activity. The Ir_2MS_2 core (M = Pd, Pt) seems to be effective for the addition of MeOH to 1-phenyl-1-propyne.

Cluster **3** also worked as a regioselective catalyst for the addition of MeOH to other internal 1-aryl-1-alkynes to give the corresponding acetals **12** in preference to **13** (Eq. (4)). Regioselective addition of EtOH to 1-phenyl-1-propyne was similarly achieved by the catalysis of **3**, although the reaction rate was lowered. In contrast to alkynes, alkenes such as styrene and 1-phenyl-1-propene did not react with MeOH at 50°C. The results of the reactions of various internal 1-aryl-1-alkynes are listed in Table 4.

Table 4
Catalytic addition of alcohols to alkynes by cluster **3** [a]

Alkyne	Alcohol	Conversion (%) [b]	Isolated yield (%)	**12**:**13** [c]
PhC≡CMe	MeOH	>99	88	98:2
PhC≡CMe	EtOH	93	89	97:3
PhC≡CEt	MeOH	>99	81	99:1
PhC≡CBu^n [d]	MeOH	>99	65	98:2
p-ClC_6H_4C≡CMe	MeOH	>99	95	97:3
m-ClC_6H_4C≡CMe	MeOH	>99	70	99:1
p-TolC≡CMe	MeOH	>99	82	91:9
p-$MeOC_6H_4C$≡CMe	MeOH	>99	59	66:34

[a] For reaction conditions, see Section 3.
[b] Determined by GLC.
[c] Determined by ^{1}H-NMR.
[d] Alkyne, 1.12 mmol (S/C = 20); 72 h.

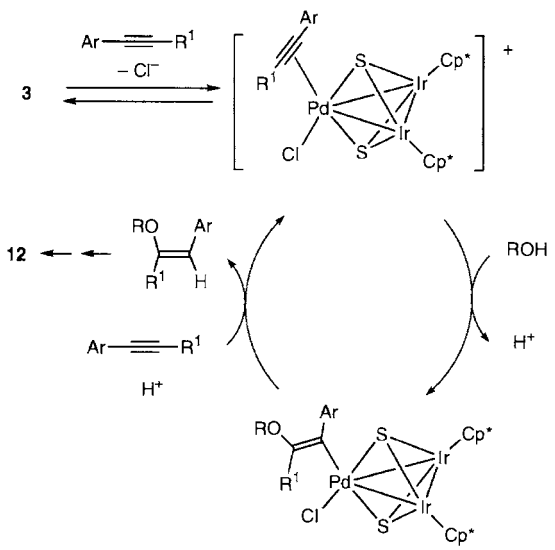

Scheme 1.

From the reactions of 1-phenyl and 1-chlorophenyl-1-alkynes, the corresponding acetals **12** were obtained in high selectivity. However, introduction of an electron donating substituent to the *p*-position of the phenyl group of the substrate alkyne decreased the regioselectivity. This observation indicates that the regiochemistry is controlled by the electronic effect of the aryl group, although the unexpectedly high regioselectivity of **3** has not been fully understood. As a related system, it has been proposed that the regiochemistry in the reaction of the cationic palladium complex $[Pd(PNP)(CH_2{=}CHPh)]^{2+}$ (PNP = 2,6-bis((diphenylphosphino)methyl)pyridine) with dimethylamine to give the benzylpalladium complex $[Pd(PNP)(CHPhCH_2NMe_2)]^+$ can be explained on steric grounds [19]. However, the selectivity of the present reaction cannot be accounted for by similar steric effects, because the reaction of phenylacetylene gave 1,1-dimethoxy-1-phenylethane predominantly (vide supra).

It is well-known that hydration of alkynes is promoted by various transition metal compounds [20]. However, the reaction of 1-phenyl-1-propyne in acetone–water (4:1) in the presence of cluster **3** resulted in recovery of the starting alkyne. Therefore, it is unlikely that the above acetal formation involves the hydration of an alkyne with fortuitous water to form the corresponding ketones followed by the condensation with MeOH. Considering the fact that the chloro ligands in **3** undergo facile substitution reactions, the catalytic cycle for the formation of **12** is presumed to be initiated by replacement of the chloro ligand at the palladium center in **3** with an alkyne molecule. However, attempts to detect an intermediate cluster formed from **3** and 1-phenyl-1-propyne were unsuccessful. The nucleophilic attack of an alcohol molecule on the coordinated alkyne followed by the protonolysis of the resultant alkoxyvinyl cluster produces a vinyl ether, which is further converted to **12** by the addition of a second alcohol molecule (Scheme 1). In fact, addition of MeOH to PhCH=C(OMe)Me was found to be catalyzed by cluster **3** to afford **12a** in 86% yield under the same conditions. Although the details of the reaction mechanism remain to be elucidated, it is noteworthy that the palladium center in the heterometallic sulfido cluster **3** works as a specifically active and regioselective reaction site for the acetal formation from nonactivated internal 1-aryl-1-alkynes and alcohols. Further studies on heterometallic sulfido clusters including **3** and **4** toward catalytic organic synthesis are under investigation.

3. Experimental

3.1. General considerations

All manipulations were performed under a nitrogen atmosphere using standard Schlenk tube techniques. Complexes **1** [6a,b] and **2** [7b,c] were prepared according to the method described previously. 1-(*p*-Chlorophenyl)-1-propyne [21], 1-(*m*-chlorophenyl)-1-propyne [21], 1-(*p*-tolyl)-1-propyne [22], 1-(*p*-methoxyphenyl)-1-propyne [21], PhCH=C(OMe)Me [23], and complexes $[PdCl_2(COD)]$ [24], $[PtCl_2(COD)]$ [24], $[PdCl_2(PhSCH_2CH_2CH_2SPh)]$ [25], $[(Ph_3P)(PhS)Pd(\mu\text{-}SPh)]_2$ [26], $[IrCl(COD)]_2$ [27], $[Cp^*IrCl(\mu\text{-}Cl)_2IrCp^*Cl]$ [28], $[(Cp^*Ru)_2Pd_2(\mu_3\text{-}S)_2(S^iPr)(\mu\text{-}S^iPr)(PPh_3)]$ [29], $[Pd(PPh_3)(\mu\text{-}S)_2\{W(S_2CNEt_2)\}_2(\mu\text{-}S)_2]$ [15], and $[Pt(PPh_3)(\mu\text{-}S)_2\{W(S_2CNEt_2)\}_2(\mu\text{-}S)_2]$ [15] were prepared by the literature methods. Solvents were dried and distilled prior to use. Other reagents were commercially obtained and used without further purification. IR spectra were recorded on a Shimadzu 8100M spectrometer. ^{1}H- and ^{13}C{^{1}H}-NMR spectra were obtained on a JEOL JNM-LA 400 spectrometer (^{1}H, 400 MHz; ^{13}C, 101 MHz), and ^{31}P{^{1}H}-NMR spectra on a JEOL EX-270 spectrometer (109 MHz). Quantitative GLC analyses of liquid products were performed on a Shimadzu GC-14A instrument equipped with a flame ionization detector using a 25 m × 0.25 mm CBP10 fused silica capillary column, while GLC analyses of gaseous products were carried out on a Shimadzu GC-8A instrument equipped with a thermal conductivity detector using a molecular sieve 13X column. Elemental analyses were performed on a Perkin–Elmer 2400II CHN analyzer. XPS analyses were carried out by using a Kratos XSAM800pci spectrometer.

3.2. Preparation of $[(Cp^*Ir)_2(\mu_3\text{-}S)_2PdCl_2]$ (3)

To a solution of complex **2** (477 mg, 0.602 mmol) in THF (20 ml) was added $[PdCl_2(COD)]$ (270 mg, 0.946 mmol), and the mixture was stirred at 50°C for 15 h. The dark green solid that deposited was collected by filtration and recrystallized from CH_2Cl_2–hexane to afford $[(Cp^*Ir)_2(\mu_3\text{-}S)_2PdCl_2]$ (**3**) as dark green crystals (399 mg, 0.445 mmol, 74% yield). ^{1}H-NMR ($CDCl_3$): δ 2.15 (s, 30H, Cp*). Anal. Calc. for $C_{20}H_{30}Cl_2Ir_2PdS_2$: C, 26.80; H, 3.37. Found: C, 26.35; H, 3.47%.

3.3. Preparation of $[(Cp^*Ir)_2(\mu_3\text{-}S)_2PtCl_2]$ (4)

To a solution of complex **2** (60 mg, 0.076 mmol) in THF (8 ml) was added $[PtCl_2(COD)]$ (34 mg, 0.091 mmol), and the mixture was stirred at 50°C for 15 h. The dark green solid that deposited was collected by filtration and recrystallized from CH_2Cl_2–ether to afford $[(Cp^*Ir)_2(\mu_3\text{-}S)_2PtCl_2]$ (**4**) as dark green crystals (48 mg, 0.049 mmol, 64% yield). ^{1}H-NMR ($CDCl_3$): δ 2.14 (s, 30H, Cp*). Anal. Calc. for $C_{20}H_{30}Cl_2Ir_2PtS_2$: C, 24.39; H, 3.07. Found: C, 24.42; H, 3.17%.

3.4. Preparation of $[(Cp^*Ir)_2(\mu_3\text{-}S)_2PdCl(PPh_3)]Cl\cdot CH_2Cl_2$ (5·CH_2Cl_2)

Complex **2** (70 mg, 0.088 mmol) and $[Pd(PPh_3)_4]$ (102 mg, 0.088 mmol) were dissolved in THF (15 ml), and the mixture was stirred at r.t. for 48 h. The solvent was removed under reduced pressure, and the residual solid was extracted with CH_2Cl_2. Addition of benzene and hexane to the concentrated extract gave $[(Cp^*Ir)_2(\mu_3\text{-}S)_2PdCl(PPh_3)]Cl\cdot CH_2Cl_2$ (**5**·CH_2Cl_2) as dark brown crystals (75 mg, 0.060 mmol, 68% yield). ^{1}H-NMR (CD_3COCD_3): δ 2.09 (s, 30H, Cp*), 7.46–7.61 (m, 15H, Ph). ^{31}P{^{1}H}-NMR (CD_3COCD_3): δ 28.2 (s). Anal. Calc. for $C_{39}H_{47}Cl_4Ir_2PPdS_2$: C, 37.67; H, 3.81. Found: C, 37.63; H, 3.82%. In a separate run, the gaseous phase was analyzed by GLC to reveal that H_2 was formed in 47% yield based on the complex **2** used.

3.5. Reactions of clusters 3 and 4 with PPh_3

To a $CDCl_3$ solution (0.65 ml) of cluster **3** (0.015 mmol) in an NMR tube was added PPh_3 (0.018 mmol) to give a greenish brown solution. The ^{1}H- and ^{31}P{^{1}H}-NMR spectra of the solution were essentially identical to those of cluster **5** except that a small amount of free PPh_3 was also detected. Further addition of PPh_3 (0.035 mmol) to this solution caused color change to red brown. The ^{1}H- and ^{31}P{^{1}H}-NMR spectra indicated the formation of a new cluster species, which is tentatively identified as $[(Cp^*Ir)_2(\mu_3\text{-}S)_2Pd(PPh_3)_2]Cl_2$ (**6**). The molar ratio of **5** and **6** in the solution was determined to be 73:27 based on the ^{31}P{^{1}H}-NMR spectrum. Selected spectral data of **6** are as follows. ^{1}H-NMR ($CDCl_3$): δ 2.09 (s, 30H, Cp*). ^{31}P{^{1}H}-NMR ($CDCl_3$): δ 20.5 (s).

Similarly, the ^{1}H- and ^{31}P{^{1}H}-NMR analysis of a green $CDCl_3$ solution containing cluster **4** (0.011 mmol) and PPh_3 (0.011 mmol) showed that ca. 80% of **4** was converted to $[(Cp^*Ir)_2(\mu_3\text{-}S)_2PtCl(PPh_3)]Cl$ (**7**). ^{1}H-NMR ($CDCl_3$): δ 2.06 (s, 30H, Cp*). ^{31}P{^{1}H}-NMR ($CDCl_3$): δ 12.7 (s, $J_{Pt-P} = 3945$ Hz). Further addition of PPh_3 (0.010 mmol) to the above solution caused rapid color change to purple, where $[(Cp^*Ir)_2(\mu_3\text{-}S)_2Pt(PPh_3)_2]Cl_2$ (**8**) was the only cluster species detected by NMR. ^{1}H-NMR ($CDCl_3$): δ 2.08 (s, 30H, Cp*). ^{31}P{^{1}H}-NMR ($CDCl_3$): δ 2.9 (s, $J_{Pt-P} = 3685$ Hz).

3.6. Preparation of $[(Cp^*Ir)_2(\mu_3\text{-}S)_2Pt(PPh_3)_2][BPh_4]_2$ (**8'**)

To a solution of **4** (35 mg, 0.036 mmol) in CH_2Cl_2 (4 ml) was added PPh_3 (25 mg, 0.095 mmol). The mixture immediately turned purple and was stirred at r.t. for 4 h. Then the solvent was removed in vacuo, $NaBPh_4$ (32 mg, 0.094 mmol) and THF (4 ml) were added to the residue, and the mixture was stirred for 15 h. The solvent was evaporated to dryness, and the residual solid was extracted with CH_2Cl_2. Addition of hexane to the concentrated extract deposited **8'** as purple needles (51 mg, 0.025 mmol, 69% yield). ^{1}H-NMR (CD_3COCD_3): δ 2.14 (s, 30H, Cp*), 6.74–7.56 (m, 70H, PPh_3 and BPh_4). $^{31}P\{^1H\}$-NMR (CD_3COCD_3): δ 4.2 (s, $J_{Pt-P} = 3684$ Hz). Anal. Calc. for $C_{104}H_{100}B_2Ir_2P_2PtS_2$: C, 60.14; H, 4.85. Found: C, 60.30; H, 4.84%.

3.7. Preparation of $[(Cp^*Ir)_2(\mu_3\text{-}S)_2Pd(dppe)][BPh_4]_2 \cdot CH_3COCH_3$ (**9**·CH_3COCH_3)

To a freshly prepared solution of **3** (50 mg, 0.056 mmol) in CH_2Cl_2 (5 ml) was added dppe (27 mg, 0.068 mmol). The color of the solution rapidly changed to dark purple. $NaBPh_4$ (191 mg, 0.558 mmol) was added to the mixture, and the solution was stirred for 20 h. The resulting mixture was filtered, and the filtrate was dried up in vacuo and dissolved in acetone. Addition of hexane to the acetone solution afforded **9**·CH_3COCH_3 as dark purple crystals (63 mg, 0.033 mmol, 59% yield). ^{1}H-NMR (CD_3COCD_3): δ 2.02 (s, 30H, Cp*), 2.94 (br d, 4H, $J = 23.1$ Hz, CH_2 of dppe), 6.76 (t, 8H, $J = 7.3$ Hz, *p*-H of BPh_4), 6.91 (t, 16H, $J = 7.3$ Hz, *m*-H of BPh_4), 7.29–7.36 (m, 16H, *o*-H of BPh_4), 7.64–7.74 (m, 20H, Ph of dppe). $^{31}P\{^1H\}$-NMR (CD_3COCD_3): δ 64.7 (s). Anal. Calc. for $C_{97}H_{100}B_2Ir_2OP_2PdS_2$: C, 60.67; H, 5.25. Found: C, 60.50; H, 5.25%.

3.8. Preparation of $[(Cp^*Ir)_2(\mu_3\text{-}S)_2Pt(dppe)][BPh_4]_2 \cdot CH_3COCH_3$ (**10**·CH_3COCH_3)

To a freshly prepared solution of **4** (100 mg, 0.102 mmol) in CH_2Cl_2 (10 ml) was added dppe (49 mg, 0.123 mmol). The color of the solution rapidly changed to dark purple. $NaBPh_4$ (174 mg, 0.508 mmol) was added to the mixture, and the solution was stirred for 20 h. The resulting mixture was filtered, and the filtrate was dried up in vacuo and dissolved in acetone. Addition of hexane to the acetone solution precipitated dark purple crystals of **10**·CH_3COCH_3 and a small amount of brown powder. The crystals of **10**·CH_3COCH_3 were collected by decantation, washed with hexane, and dried in vacuo (90 mg, 0.045 mmol, 44% yield). ^{1}H-NMR (CD_3COCD_3): δ 2.03 (s, 30H, Cp*), 2.91 (br d, 4H, $J = 19.5$ Hz, CH_2 of dppe), 6.76 (t, 8H, $J = 7.1$ Hz, *p*-H of BPh_4), 6.90 (t, 16H, $J = 7.1$ Hz, *m*-H of BPh_4), 7.29–7.36 (m, 16H, *o*-H of BPh_4), 7.63–7.72 (m, 20H, Ph of dppe). $^{31}P\{^1H\}$-NMR (CD_3COCD_3): δ 49.4 (s, $J_{Pt-P} = 3517$ Hz). Anal. Calc. for $C_{97}H_{100}B_2Ir_2OP_2PtS_2$: C, 57.99; H, 5.02. Found: C, 57.59; H, 5.24%.

3.9. Preparation of $[(Cp^*Ir)_2(\mu_3\text{-}S)_2PtCl(CN^tBu)][PF_6]$ (**11**)

To an acetone solution (5 ml) of complex **4** (50 mg, 0.051 mmol) was added CN^tBu (6 μl, 0.05 mmol), and the mixture was stirred for 2 h at r.t. KPF_6 (10 mg, 0.054 mmol) was added to the solution, and the solution was stirred for further 30 min. The resultant green solution was filtered and evaporated in vacuo, and the residual solid was recrystallized from acetone–hexane to give **11** as green needles (24 mg, 20 mmol, 40% yield). ^{1}H-NMR (CD_3COCD_3): δ 2.12 (s, 30H, Cp*), 1.49 (s, 9H, ^{t}Bu). IR (KBr) ν(CN) 2203 cm^{-1}. Anal. Calc. for $C_{25}H_{39}ClF_6Ir_2NPPtS_2$: C, 25.50; H, 3.34; N, 1.19. Found: C, 25.89; H, 3.32; N, 1.40%.

3.10. Catalytic addition of alcohols to alkynes

The following procedure for the addition of MeOH to 1-phenyl-1-propyne is representative. 1-Phenyl-1-propyne (1.67 mmol) and a catalytic amount of cluster **3** (56 μmol, S/C = 30) were dissolved in MeOH (2 ml), and the solution was stirred at 50°C for 48 h. Then, NEt_3 (0.1 ml) was added to the reaction mixture in order to prevent hydrolysis of the products, and the mixture was analyzed by GLC, which showed that 2,2-dimethoxy-1-phenylpropane (**12a**) and 1,1-dimethoxy-1-phenylpropane (**13a**) were formed in the ratio of 98:2. The mixture was evaporated under reduced pressure, and the residue was dissolved in ether and passed through a silica gel column (eluent, ether). A small amount of K_2CO_3 was added to the eluate, and the solvent was removed under reduced pressure. Bulb-to-bulb distillation of the residual oil gave a 98:2 mixture of **12a** and **13a** as a colorless oil (88% yield). **12a**. ^{1}H-NMR: δ 1.12 (s, 3H, Me), 2.90 (s, 2H, CH_2), 3.24 (s, 6H, OMe), 7.16–7.24 (m, 5H, Ph). $^{13}C\{^1H\}$-NMR: δ 20.9, 42.7, 48.0, 101.6, 126.1, 127.8, 130.0, 137.3. **13a**. ^{1}H-NMR: δ 0.58 (t, 3H, $J = 7.8$ Hz, Me), 1.90 (q, 2H, $J = 7.8$ Hz, CH_2), 3.12 (s, 6H, OMe). The aromatic signals could not be assigned because of overlapping with those of **12a**.

Acetals **12b**–**h** and **13b**–**h** were obtained by similar procedures. Selected spectral data are as follows.

3.10.1. 2,2-Diethoxy-1-phenylpropane (**12b**)

^{1}H-NMR: δ 1.15 (s, 3H, Me), 1.21 (t, 6H, $J = 7.3$ Hz, OCH_2Me), 2.94 (s, 2H, CH_2Ph), 3.55 (m, 4H, OCH_2), 7.17–7.32 (m, 5H, Ph). $^{13}C\{^1H\}$-NMR: δ 15.4, 22.1, 43.8, 55.7, 101.5, 126.1, 127.8, 130.2, 137.7.

*3.10.2. 1,1-Diethoxy-1-phenylpropane (**13b**)*

^{1}H-NMR: δ 0.57 (t, 3H, $J = 6.9$ Hz, Me), 1.92 (q, 2H, $J = 6.9$ Hz, CCH_2Me). The ethoxy and aromatic signals could not be assigned because of overlapping with those of **12b**.

*3.10.3. 2,2-Dimethoxy-1-phenylbutane (**12c**)*

^{1}H-NMR: δ 0.85 (t, 3H, $J = 7.6$ Hz, Me), 1.46 (q, 2H, $J = 7.6$ Hz, CH_2Me), 2.90 (s, 2H, CH_2Ph), 3.26 (s, 6H, OMe), 7.18–7.24 (m, 5H, Ph). ^{13}C{^{1}H}-NMR: δ 7.9, 25.1, 37.7, 47.8, 103.9, 126.1, 128.0, 129.7, 136.9.

*3.10.4. 1,1-Dimethoxy-1-phenylbutane (**13c**)*

^{1}H-NMR: δ 1.00 (t, 3H, $J = 7.2$ Hz, Me), 1.85 (pseudo t, 2H, $J = 7.7$ Hz, CH_2C(OMe)$_2$), 3.13 (s, 6H, OMe). The methylene and aromatic signals could not be assigned because of overlapping with those of **12c**.

*3.10.5. 2,2-Dimethoxy-1-phenylhexane (**12d**)*

^{1}H-NMR: δ 0.83 (t, 3H, $J = 6.9$ Hz, Me), 1.18–1.39 (m, 6H, (CH$_2$)$_3$), 2.91 (s, 2H, CH_2Ph), 3.27 (s, 6H, OMe), 7.15–7.32 (m, 5H, Ph). ^{13}C{^{1}H}-NMR: δ 13.9, 22.7, 25.7, 32.3, 38.3, 47.9, 103.6, 126.2, 128.1, 129.8, 137.3.

*3.10.6. 1,1-Dimethoxy-1-phenylhexane (**13d**)*

^{1}H-NMR: δ 0.95 (t, 3H, $J = 8.6$ Hz, Me), 1.85 (pseudo t, 2H, $J = 8.3$ Hz, CH_2C(OMe)$_2$), 3.15 (s, 6H, OMe). The methylene and aromatic signals could not be assigned because of overlapping with those of **12d**.

*3.10.7. 2,2-Dimethoxy-1-(p-chlorophenyl)propane (**12e**)*

^{1}H-NMR: δ 1.10 (s, 3H, Me), 2.86 (s, 2H, CH$_2$), 3.24 (s, 6H, OMe), 7.15 (d, 2H, $J = 8.4$ Hz, aryl), 7.22 (d, 2H, $J = 8.4$ Hz, aryl). ^{13}C{^{1}H}-NMR: δ 20.9, 42.1, 48.1, 101.3, 128.0, 131.4, 132.0, 135.8.

*3.10.8. 1,1-Dimethoxy-1-(p-chlorophenyl)propane (**13e**)*

^{1}H-NMR: δ 0.56 (t, 3H, $J = 7.7$ Hz, Me), 1.87 (q, 2H, $J = 7.7$ Hz, CH$_2$), 3.12 (s, 6H, OMe). The aromatic signals could not be assigned because of overlapping with those of **12e**.

*3.10.9. 2,2-Dimethoxy-1-(m-chlorophenyl)propane (**12f**)*

^{1}H-NMR: δ 1.13 (s, 3H, Me), 2.88 (s, 2H, CH$_2$), 3.25 (s, 6H, OMe), 7.10–7.24 (m, 4H, aryl). ^{13}C{^{1}H}-NMR: δ 21.0, 42.5, 48.3, 101.4, 126.4, 128.3, 129.2, 130.2, 133.7, 139.5.

*3.10.10. 1,1-Dimethoxy-1-(m-chlorophenyl)propane (**13f**)*

^{1}H-NMR: δ 0.58 (t, 3H, $J = 7.2$ Hz, Me), 1.88 (q, 2H, $J = 7.2$ Hz, CH$_2$), 3.15 (s, 6H, OMe). The aromatic signals could not be assigned because of overlapping with those of **12f**.

*3.10.11. 2,2-Dimethoxy-1-(p-tolyl)propane (**12g**)*

^{1}H-NMR: δ 1.13 (s, 3H, Me), 2.30 (s, 3H, C$_6$H$_4$*Me*), 2.87 (s, 2H, CH$_2$), 3.25 (s, 6H, OMe), 7.07 (d, 2H, $J = 8.3$ Hz, aryl), 7.12 (d, 2H, $J = 8.3$ Hz, aryl). ^{13}C{^{1}H}-NMR: δ 20.88, 20.94, 42.2, 48.1, 101.7, 128.6, 129.9, 134.2, 135.6.

*3.10.12. 2,2-Dimethoxy-1-(p-tolyl)propane (**13g**)*

^{1}H-NMR: δ 0.59 (t, 3H, $J = 7.7$ Hz, Me), 1.91 (q, 2H, $J = 7.7$ Hz, CH$_2$), 2.33 (s, 3H, C$_6$H$_4$*Me*), 3.14 (s, 6H, OMe). The aromatic signals could not be assigned because of overlapping with those of **12g**.

*3.10.13. 2,2-Dimethoxy-1-(p-methoxyphenyl)propane (**12h**)*

^{1}H-NMR: δ 1.12 (s, 3H, Me), 2.84 (s, 2H, CH$_2$), 3.25 (s, 6H, C(OMe)$_2$), 3.75 (s, 3H, C$_6$H$_4$O*Me*), 6.80 (d, 2H, $J = 8.6$ Hz, aryl), 7.13 (d, 2H, $J = 8.6$ Hz, aryl). ^{13}C{^{1}H}-NMR:δ 21.7, 42.5, 48.9, 55.8, 102.5, 114.1, 131.7, 133.4, 159.6.

*3.10.14. 1,1-Dimethoxy-1-(p-chlorophenyl)propane (**13h**)*

^{1}H-NMR: δ 0.58 (t, 3H, $J = 7.3$ Hz, Me), 1.87 (q, 2H, $J = 7.3$ Hz, CH$_2$), 3.12 (s, 6H, C(OMe)$_2$), 3.77 (s, 3H, C$_6$H$_4$O*Me*), 6.85 (d, 2H, $J = 8.9$ Hz, aryl), 7.30 (d, 2H, $J = 8.9$ Hz, aryl). ^{13}C{^{1}H}-NMR: δ 8.4, 30.5, 49.1, 55.8, 104.7, 113.8, 128.9, 130.1, 159.7.

3.11. X-ray crystallographic studies

Single crystals of **5**·CH_2Cl_2, **9**·CH_3COCH_3, and **10**·CH_3COCH_3 were sealed in glass capillaries under an argon atmosphere and used for data collection. Diffraction data were collected on a Rigaku AFC7R four-circle automated diffractometer with graphite-monochromatized Mo–K_α radiation ($\lambda = 0.71069$ Å) at 21°C using the ω–2θ scan technique for **5**·CH_2Cl_2 ($5 < 2\theta < 55°$) and the ω scan technique for **9**·CH_3COCH_3 and **10**·CH_3COCH_3 ($5 < 2\theta < 50°$). Intensity data were corrected for Lorentz and polarization effects and for absorption (empirical, ω scans). For crystals of **5**·CH_2Cl_2, no significant decay was observed for three standard reflections monitored every 150 reflections during the data collection. For compounds **9**·CH_3COCH_3 and **10**·CH_3COCH_3, a slight decay (**9**·CH_3COCH_3, 1.81%; **10**·CH_3COCH_3, 6.57%) was observed during the data collection, and a correction for decay was applied in each case.

The structure solution and refinements were carried out by using the TEXSAN crystallographic software package [30]. The positions of the non-hydrogen atoms were determined by Patterson methods (DIRDIF PATTY [31]) and subsequent Fourier syntheses. The carbon atoms of the phenyl groups in the dppe ligands of **10**·CH_3COCH_3 were refined with isotropic thermal

Table 5
X-ray crystallographic data for $\mathbf{5}\cdot CH_2Cl_2$, $\mathbf{9}\cdot CH_3COCH_3$, and $\mathbf{10}\cdot CH_3COCH_3$

	$\mathbf{5}\cdot CH_2Cl_2$	$\mathbf{9}\cdot CH_3COCH_3$	$\mathbf{10}\cdot CH_3COCH_3$
Formula	$C_{39}H_{47}Cl_{14}Ir_2PPdS_2$	$C_{97}H_{100}B_2Ir_2OP_2PdS_2$	$C_{97}H_{100}B_2Ir_2OP_2PtS_2$
Formula weight	1243.55	1920.38	2009.07
Crystal system	Monoclinic	Monoclinic	Monoclinic
Space group	$P2_1/m$	$P2_1/n$	$P2_1/n$
Crystal size (mm)	$0.40\times0.40\times0.15$	$0.50\times0.40\times0.30$	$0.40\times0.25\times0.20$
a (Å)	12.021(2)	14.725(4)	14.754(3)
b (Å)	12.542(3)	22.400(3)	22.444(3)
c (Å)	14.667(2)	26.877(3)	26.854(3)
β (°)	93.02(1)	103.67(1)	103.58(1)
V (Å^3)	2208.3(6)	8614(2)	8643(2)
Z	2	4	4
μ(Mo–K$_\alpha$) (cm^{-1})	68.29	34.29	48.20
Unique reflections	5306 [$R_{int}=0.031$]	15103 [$R_{int}=0.046$]	15145 [$R_{int}=0.045$]
Observed reflections	3572 ($I>3\sigma(I)$)	7276 ($I>3\sigma(I)$)	6604 ($I>3\sigma(I)$)
Number of variables	239	929	808
R [a]	0.048	0.045	0.066
R_w [b]	0.042	0.027	0.048
Goodness-of-fit [c]	2.63	1.54	1.93

[a] $R=\Sigma||F_o|-|F_c||/\Sigma|F_o|$.
[b] $R_w=[\Sigma w(|F_o|-|F_c|)^2/\Sigma wF_o^2]^{1/2}$, $w=[\sigma_c^2(F_o)+p^2F_o^2/4]^{-1}$.
[c] GOF $=[\Sigma w(|F_o|-|F_c|)^2/(N_{obs}-N_{params})]^{1/2}$.

parameters, and fixed isotropic parameters were used for the carbon and oxygen atoms of the acetone molecules in $\mathbf{9}\cdot CH_3COCH_3$ and $\mathbf{10}\cdot CH_3COCH_3$. The other non-hydrogen atoms were refined by full-matrix least-squares techniques (based on F) with anisotropic thermal parameters. Hydrogen atoms except for those of the acetone molecules in $\mathbf{9}\cdot CH_3COCH_3$ and $\mathbf{10}\cdot CH_3COCH_3$ were placed at the calculated positions ($d_{C-H}=0.95$ Å) and were included with fixed isotropic parameters. Reinvestigation of the crystal structure of $\mathbf{5}\cdot CH_2Cl_2$, which is reported herein, gave slightly different cell parameters from those described previously [7b], but the molecular structure obtained was essentially the same. Details of the X-ray diffraction study are summarized in Table 5.

4. Supplementary material

Crystallographic data for this structural analysis have been deposited with the Cambridge Crystallographic Data Centre, CCDC no. 146339 (compound $\mathbf{5}\cdot CH_2Cl_2$), no. 146340 (compound $\mathbf{9}\cdot CH_3COCH_3$), and no. 146341 (compound $\mathbf{10}\cdot CH_3COCH_3$). Copies of this information may be obtained free of charge from The Director, CCDC, 12 Union Road, Cambridge, CB2 1EZ, UK (Fax. +44-1223-336-033, or e-mail: deposit@ccdc.cam.ac.uk or http://www.ccdc.cam.ac.uk).

Acknowledgements

This work was supported by a Grant-in-aid for Specially Promoted Research (09102004) from the Ministry of Education, Science, Sports, and Culture, Japan.

References

[1] (a) R.D. Adams, F.A. Cotton (Eds.), Catalysis by Di and Polynuclear Metal Cluster Complexes, Wiley, New York, 1998. (b) G. Süss-Fink, G. Meister, Adv. Organomet. Chem. 35 (1993) 41.
[2] (a) R.H. Holm, S. Ciurli, J.A. Weigel, Prog. Inorg. Chem. 38 (1990) 1. (b) B. Krebs, G. Henkel, Angew. Chem. Int. Ed. Engl. 30 (1991) 769. (c) T. Shibahara, Coord. Chem. Rev. 123 (1993) 73. (d) T. Saito, in: M.H. Chisholm (Ed.), Early Transition Metal Clusters with π-Donor Ligands, VCH, New York, 1995, chapter 3. (e) I. Dance, K. Fisher, Prog. Inorg. Chem. 41 (1994) 637. (f) P. Mathur, Adv. Organomet. Chem. 41 (1997) 243. (g) H. Ogino, S. Inomata, H. Tobita, Chem. Rev. 98 (1998) 2093.
[3] (a) M. Rakowski DuBois, Chem. Rev. 89 (1989) 1. (b) J.C. Bayón, C. Claver, A.M. Masdeu-Bultó, Coord. Chem. Rev. 193–195 (1999) 73.
[4] (a) M. Hidai, Y. Mizobe, H. Matsuzaka, J. Organomet. Chem. 473 (1994) 1. (b) M. Hidai, Y. Mizobe, in: E.I. Stiefel, K. Matsumoto (Eds.), Transition Metal Sulfur Chemistry: Biological and Industrial Significance, ACS Symposium Series 653, American Chemical Society, Washington, DC, 1996, p. 310. (c) M. Hidai, S. Kuwata, Y. Mizobe, Acc. Chem. Res. 33 (2000) 46.
[5] (a) T. Ikada, S. Kuwata, Y. Mizobe, M. Hidai, Inorg. Chem. 38 (1999) 64. (b) T. Amemiya, S. Kuwata, M. Hidai, Chem. Commun. (1999) 711. (c) T. Iwasa, H. Shimada, A. Takami, H. Matsuzaka, Y. Ishii, M. Hidai, Inorg. Chem. 38 (1999) 2851. (d)

S. Matsukawa, S. Kuwata, M. Hidai, Inorg. Chem. 39 (2000) 791.
[6] (a) T. Murata, H. Gao, Y. Mizobe, F. Nakano, S. Motomura, T. Tanase, S. Yano, M. Hidai, J. Am. Chem. Soc. 114 (1992) 8287. (b) T. Murata, Y. Mizobe, H. Gao, Y. Ishii, T. Wakabayashi, F. Nakano, T. Tanase, S. Yano, M. Hidai, I. Echizen, H. Nanikawa, S. Motomura, J. Am. Chem. Soc. 116 (1994) 3389. (c) T. Wakabayashi, Y. Ishii, T. Murata, Y. Mizobe, M. Hidai, Tetrahedron Lett. 36 (1995) 5585. (d) T. Wakabayashi, Y. Ishii, K. Ishikawa, M. Hidai, Angew. Chem. Int. Ed. Engl. 35 (1996) 2123.
[7] (a) K. Hashizume, Y. Mizobe, M. Hidai, Organometallics 15 (1996) 3303. (b) Z. Tang, Y. Nomura, Y. Ishii, Y. Mizobe, M. Hidai, Organometallics 16 (1997) 151. (c) Z. Tang, Y. Nomura, Y. Ishii, Y. Mizobe, M. Hidai, Inorg. Chim. Acta 267 (1998) 73.
[8] (a) S. Kuwata, M. Hidai, Chem. Lett. (1998) 885. (b) S. Kabashima, S. Kuwata, M. Hidai, J. Am. Chem. Soc. 121 (1999) 7837.
[9] (a) S. Kuwata, M. Andou, K. Hashizume, Y. Mizobe, M. Hidai, Organometallics 17 (1998) 3429. (b) Z. Tang, Y. Nomura, S. Kuwata, Y. Ishii, Y. Mizobe, M. Hidai, Inorg. Chem. 37 (1998) 4909. (c) T. Kochi, Y. Nomura, Z. Tang, Y. Ishii, Y. Mizobe, M. Hidai, J. Chem. Soc. Dalton Trans. (1999) 2575. (d) S. Kabashima, S. Kuwata, K. Ueno, M. Shiro, M. Hidai, Angew. Chem. Int. Ed. 39 (2000) 1128.
[10] D. Masui, Y. Ishii, M. Hidai, Chem. Lett. (1998) 717.
[11] (a) Y. Fukuda, K. Utimoto, J. Org. Chem. 56 (1991) 3729. (b) J.H. Teles, S. Brode, M. Chabanas, Angew. Chem. Int. Ed. 37 (1998) 1415. (c) Y. Kataoka, O. Matsumoto, K. Tani, Organometallics 15 (1996) 5246. (d) C. Gemel, G. Trimmel, C. Slugovc, S. Kremel, K. Mereiter, R. Schmid, K. Kirchner, Organometallics 15 (1996) 3998.
[12] S. Kuwata, Y. Mizobe, M. Hidai, unpublished results.
[13] A.L. Balch, V.J. Catalano, Inorg. Chem. 31 (1992) 2569.
[14] D.M.P. Mingos, A.S. May, in: D.F. Shriver, H.D. Kaesz, R.D. Adams (Eds.), The Chemistry of Metal Cluster Complexes, VCH, New York, 1990.
[15] T. Ikada, S. Kuwata, Y. Mizobe, M. Hidai, Inorg. Chem. 37 (1998) 5793.
[16] C.S. Bahn, A. Tan, S. Harris, Inorg. Chem. 37 (1998) 2770.
[17] N.M. Boag, M. Green, J.L. Spencer, F.G.A. Stone, J. Chem. Soc. Dalton Trans. (1980) 1220.
[18] M. Tokunaga, Y. Wakatsuki, Angew. Chem. Int. Ed. Engl. 37 (1998) 2867.
[19] C. Hahn, A. Vitagliano, F. Giordano, R. Taube, Organometallics 17 (1998) 2060.
[20] (a) W.D. Harman, J.C. Dobson, H. Taube, J. Am. Chem. Soc. 111 (1989) 3061. (b) W. Hiscox, P.W. Jennings, Organometallics 9 (1990) 1997. (c) M.M. Taqui Khan, S.B. Halligudi, S. Shukla, J. Mol. Catal. 58 (1990) 299. (d) J. Blum, H. Huminer, H. Alper, J. Mol. Catal. 75 (1992) 153. (e) J.W. Hartman, W. Hiscox, P.W. Jennings, J. Org. Chem. 58 (1993) 7613. (f) I.K. Meier, J.A. Marsella, J. Mol. Catal. 78 (1993) 31. (g) J. Yadav, S.K. Das, S. Sarkar, J. Am. Chem. Soc. 119 (1997) 4315.
[21] E.J. Corey, P.L. Fuchs, Tetrahedron Lett. 36 (1972) 3769.
[22] B. Floris, E. Tassoni, Organometallics 13 (1994) 4746.
[23] H.O. House, V. Kramar, J. Org. Chem. 28 (1963) 3362.
[24] D. Drew, J.R. Doyle, Inorg. Synth. 28 (1990) 346.
[25] F.R. Hartley, S.G. Murray, W. Levason, H.E. Soutter, C.A. McAuliffe, Inorg. Chim. Acta 35 (1979) 265.
[26] R. Zanella, R. Ros, M. Graziani, Inorg. Chem. 12 (1973) 2736.
[27] J.L. Herde, J.C. Lambert, C.V. Senoff, Inorg. Synth. 15 (1974) 18.
[28] C. White, A. Yates, P.M. Maitlis, Inorg. Synth. 29 (1992) 228.
[29] S. Kuwata, Y. Mizobe, M. Hidai, J. Am. Chem. Soc. 115 (1993) 8499.
[30] TEXSAN: Crystal Structure Analysis Package, Molecular Structure Corp., The Woodlands, TX, 1985 and 1992.
[31] PATTY: P.T. Beurskens, G. Admiraal, G. Beurskens, W.P. Bosman, S. Garcia-Granda, R.O. Gould, J.M.M. Smits, C. Smykalla, The DIRDIF program system, Technical Report of the Crystallography Laboratory, University of Nijmegen: Nijmegen, The Netherlands, 1992.